Numerical Computation of SAR in Human Head with Transparent Shields Using Transmission Line Method

Pudipeddi Sai Spandana* **and Pappu V. Y. Jayasree**

Abstract—The tremendous proliferation of mobile smartphone handsets and their usage worldwide makes human life comfortable, while the radiation hazards associated with them are alarming, especially among children. There is a necessity to minimize the Electro Magnetic Field (EMF) radiation levels. For the evaluation of Radio Frequency (RF) radiation from the mobile phone, one of the dosimetric parameters used is the Specific Absorption Rate (SAR). The RF radiation can be mitigated by incorporating a barrier or a shield of suitable material in the mobile handset design. In the proposed work, the analysis of SAR evaluation absorbed by the human head is determined with the performance of the shielding material called Shielding Effectiveness (SE) using Transmission Line Method (TLM) mathematically. The proposed shielding materials are composed of flexible and transparent thin films. Flexible and transparent thin shielding materials are advantageous over the other shielding materials in reduced size, less weight, non-corrosiveness, and easy processing. These materials include highly conductive Silver film, Silver Nanowire (AgNW) doped with PDDA (poly(diallyldimethyl-ammonium chloride)) polymer single shields, and a laminated shield comprising AgNW/PDDA with PEDOT:PSS (poly(3,4-ethylenedioxythiophene)poly-styrene sulfonate) polymer as lamination. The SARs of planar multi-layered human head models for different ages are estimated at various mobile frequencies with these shields. Under four-layered head models at 6 GHz, adult and child heads absorb 0.0006 W/kg and 0.000024 W/kg of RF radiation using pristine Silver film as a single shield. Using a single shield of Ag nanowire and PDDA, the adult and child heads absorb SARs of 0.00058 W/kg and 0.000023 W/kg, respectively. With the laminated shield of AgNW/PDDA and PEDOT:PSS as coating material, the same models are exposed to minimal amounts of 0.00054 W/kg and 0.000012 W/Kg of SAR. At 6 GHz frequency, under seven-layered head models, adult and child heads absorb 0.000047 W/kg and 0.000002 W/kg of power, respectively, using Ag film. With AgNW/PDDA shield, the adult and child heads absorb SARs of 0.000046 W/kg and 0.0000019 W/kg, respectively. The SAR of 0.000043 W/kg and a negligible value of 0.0000018 W/kg are absorbed by adult and child heads individually with the help of AgNW/PDDA/PEDOT:PSS laminated shield. The results exhibit a significant amount of reduction in Specific Absorption Rate with transparent shielding materials compared to SAR absorbed by the head without any shield. This maximum RF exposure rate reduction from mobile phones with the Ag Nanowire/PDDA/PEDOT:PSS laminated shield is achieved for a seven-layered child head model.

1. INTRODUCTION

The electromagnetic dosimetry gives the dependence of induced fields on the biological body and the distribution of an electromagnetic field in free space. The biological effects of electromagnetic radiation on living cells can be classified into ionizing and non-ionizing effects, based on the capability of radiation to ionize atoms and break chemical bonds. The non-ionizing effect raises the temperature in human

tissues. The only influence that electromagnetic radiation has on human tissues is the non-ionizing effect when the source frequency is between $100\,\text{kHz}$ and $300\,\text{GHz}$. The exposure conditions and the characteristics of the incident EMF wave have resulted in the implementation of the concept of SAR as a measure of exposure to EMF. The SAR quantifies the energy is absorbed in human tissues at the RF spectrum [1], averaged over $1\,\text{g}$ or $10\,\text{g}$ of tissue. The SAR depends on the tissue conductivity (σ), the mass density of the tissue (ρ), and the electric field intensity (E) induced in the tissue, expressed in units of W/kg. The general formula for SAR measurement is given by:

$$SAR = \frac{\sigma E^2}{2\rho} \tag{1}$$

The regulatory compliance for the standardized SAR limit of $1.6\,\text{W/kg}$ set by the Federal Communication Commission (FCC) is accepted by most countries [2].

The process of limiting the EM field flow between the mobile phone and the head can take place with a single layer of shield material called a single shield or with two or more layers stacked together called a laminated shield. Keeping in view the lightweight property of the mobile device and the minimal size of the shield, the shielding material adopted for the proposed analysis is flexible and transparent. Networks of metal nanowires are a substitute for Transparent Conductive Films (TCFs), which provide an improvement in the conductivity, do not change their shielding properties, and remain intact under flexing [3]. Nowadays, it is a pressing priority for any electronic gadget. The silver nanowires are reinforced with polymer composites to enhance the electrical conductivity of the composite film formed as a function of metal nanowire content for the formation of transparent conductive composite films.

In the literature review reported recently under transparent and flexible shielding materials, Yang et al. in [4] have made an approach to enhance the conductivity and stability of metal nanowires synthesized by reduced GO nanosheets on AgNWs in the X-band range. The shielding effectiveness of $35.3\,\text{dB}$ was exhibited using the Scattering parameters method, and the thickness achieved was $31\,\text{nm}$. Wan et al. in [5] and Chen et al. in [6] have achieved shielding effectiveness of densified CNT film and cellulose nanofibre/silver nanowire conductive paper at around $51\,\text{dB}$ and $39.3\,\text{dB}$, respectively using S-parameters method only.

Recently, Alibakhshikenari et al. have explained the design practicality and applications of composite right-handed/left-handed metamaterial-based transmission lines in antenna systems to enhance their performance parameters in dimension, radiation pattern, gain, and efficiency extending over a wide range of frequency band [7–9]. Alibakhshi-Kenari et al. have proposed an ultrawideband printed CRLH-TL metamaterial antenna for a mobile handset with improved radiation efficiency characteristics and miniaturized size [10]. Ojaroudi et al. in [11] have reported a design of a wide radiation coverage for 5G smartphone applications wherein antenna array consisted of diamond-ring slot elements with improved impedance bandwidth, good isolation and gain characteristics. Specifically for the MIMO application of mobile smartphones, the total active reflection coefficient and envelope correlation coefficient were very low.

In the literature of recent times under the Specific Absorption Rate absorbed by various human head models, the long-term exposure of radiation on the human head by analyzing SAR reduction for voice calling, messaging, and video calling features for GSM 900 and 1800 bands for only one adult head model was suggested by Tamim et al. in [12]. The authors of the article Belrhiti et al. in [13] have reported SAR with four different adult human head models exposed to radiation for Wireless LAN applications. For carrying out SAR assessment, software simulation tools were used in the reported literature.

The novelty of the proposed research is to mitigate the EM radiation due to mobile phone radiation exposure of the human head. For this purpose, suitable transparent shields based on their shielding performance or effectiveness for the mobile phone are selected. The Specific Absorption Rate is calculated numerically in the human heads of an adult and a child at different mobile frequencies both in the absence and presence of different transparent thin films (single and laminated shields) using theoretical and mathematical analysis of Transmission Line Method as the SAR is not measured using this method in the previously reported literature. The internal structure of the mobile-phone antenna design and its performance remain unaffected throughout the analysis. The head models used in this work are planar multi-layered because the human head model is considered circular, and at a point of contact of the mobile phone, the arc in the circumference of the circle looks like a straight line.

Furthermore, the proposed work focuses on transparent shielding materials and SAR estimation by considering the worst-case/normal incidence of the RF field. The simulations for planar layered head models are performed using MATLAB R2021a.

2. THEORETICAL ANALYSIS

2.1. Layered Head Models of an Adult and a Child for the Estimation of Shielding Effectiveness of the Human Head

Case A: When the Shield Is not Considered: For the theoretical analysis of shielding effectiveness of planar multi-layered head models of an adult and a child, an adult aged 50 years and a child aged 8 years are considered. The head models are considered to have the following four layers or tissues: Skin Dry, Bone Cortical, Brain Gray Matter, and Brain White Matter, and following seven layers: Skin Dry, Fat, Bone Cortical, Dura, Cerebrospinal Fluid (CSF), Brain Gray Matter, and Brain White Matter. The thicknesses of the tissues in the head models of an adult [14] and a child [15, 16] are indicated in Fig. 1 and Fig. 2. The dimensions of an adult four-layered head model with tissues are shown in Fig. 3. The total head diameter for an adult head model is 14.4 cm.
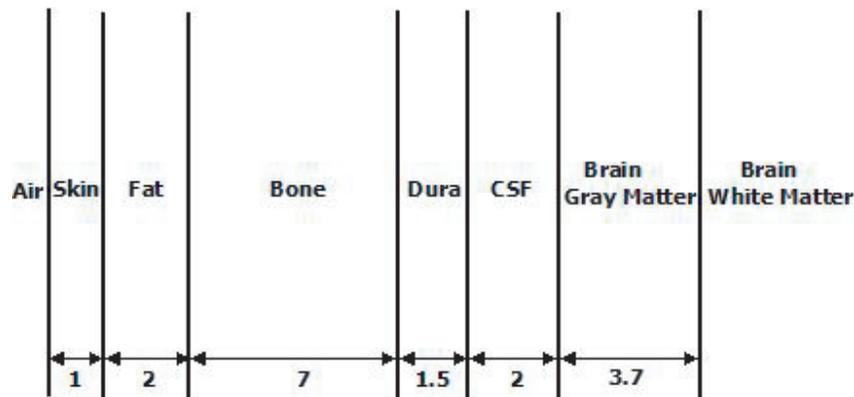
Figure 1. Thicknesses of head tissues in a planar four and a seven-layered adult head in millimetres.
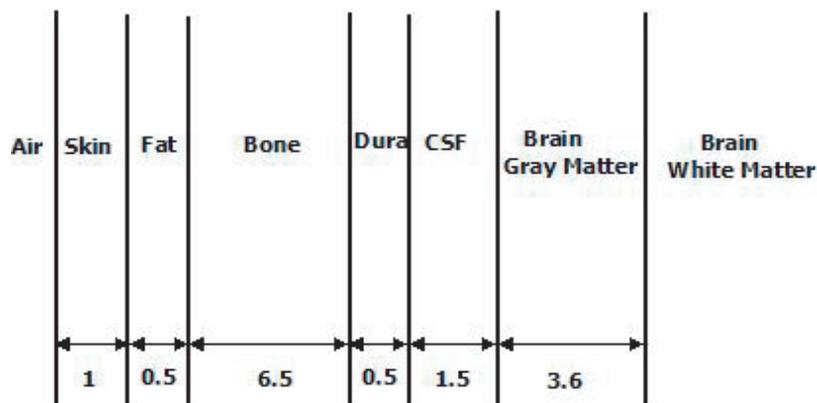
Figure 2. Thicknesses of head tissues in a planar four and a seven-layered child head in millimetres.

The head size for the child model is also taken in a similar way to the head dimensions of the adult head model. Human head tissues have values of dielectric properties dependent on frequency, geometry,
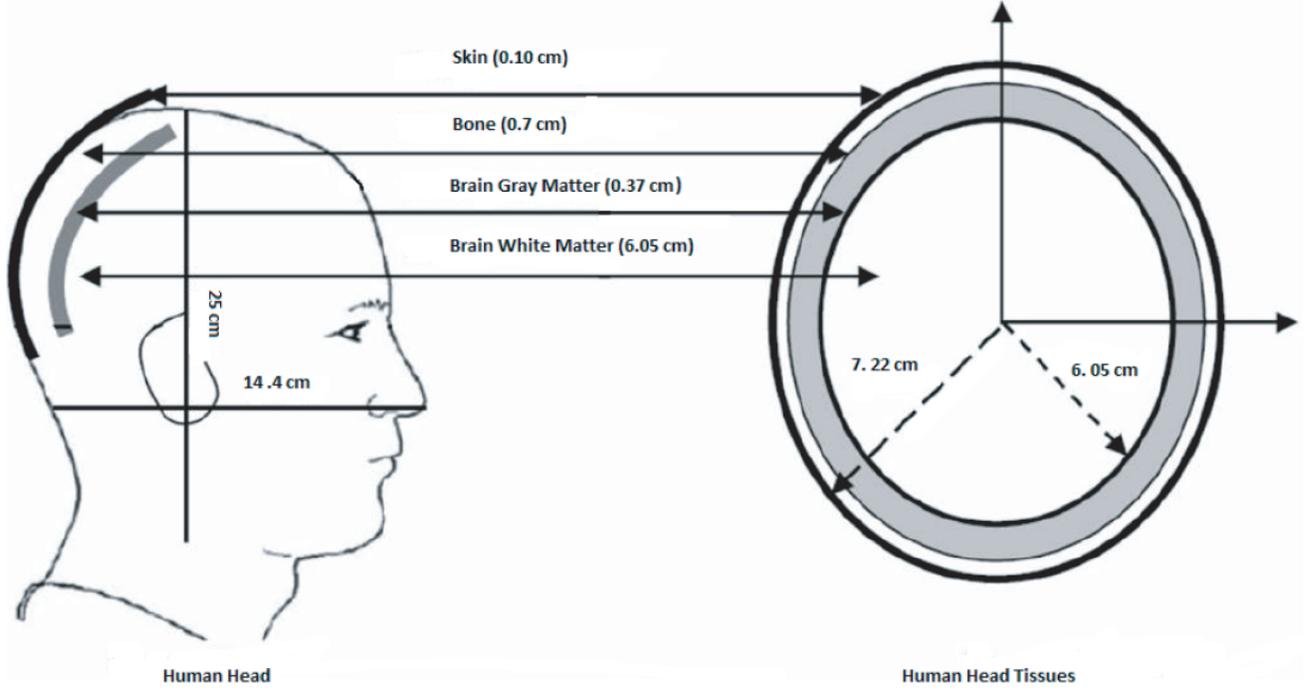
Figure 3. Head dimensions with tissues for an adult four-layered human head.

and size of tissues and water contents [16]. The variation of complex relative permittivity as a function of frequency for head tissues in an adult is obtained through Cole-Cole dispersion equation [17].

$$\varepsilon\left(\hat{\omega}\right) = \varepsilon_\infty + \sum_{n=1}^{4} \frac{\Delta\varepsilon_n}{1 + (j\omega\tau_n)^{(1-\alpha_n)}} + \frac{\sigma_i}{j\omega\varepsilon_0} \tag{2}$$

where $n = 1 - 4$ range for fitting parameters of tissues. α is a measure of broadening of dispersion. τ is the polarization time constant of relaxation regions of dielectric spectrum of tissue. σ_i is the static ionic conductivity. ε_∞ is the permittivity at high frequencies. ε_s is the permittivity at low frequencies. $\Delta\varepsilon_n$ is the magnitude of dispersion. ε_0 is the permittivity of free space.

The values of fitting parameters of tissues are obtained from [18]. The other dielectric property is the conductivity of tissues in the adult head in variation with mobile frequencies from [19].

$$\sigma = \frac{\varepsilon_0\,\varepsilon_{\rm r}}{\tau} \tag{3}$$

For finding the dielectric properties of a child's head, the age-dependent dielectric parameters of biological tissues are collected. As described in [20], the relaxation time constant is almost independent of age. Thus, at least one parameter out of relative permittivity or conductivity of biological tissue has to be known, and the other can be calculated using Eq. (3). The dielectric properties of tissues depend on tissue composition. Human biological tissues are constituted mainly by water, and each biological tissue is considered to be composed of water and organ-specific tissue. For simplification, it is assumed that the organ-specific part is not dependent on age, and the central part of biological tissue is the Total Body Water (TBW) that changes as a function of age [21].

$$\mathrm{TBW_{ch}}\text{ in }\left(\frac{\mathrm{L}}{\mathrm{kg}}\right) = \frac{0.0846\,(\mathrm{Height} * \mathrm{Weight})^{0.65}}{\mathrm{Weight}} \tag{4}$$

The height and weight of an 8-year-old child for finding TBW are obtained from [22]. TBW in (L/kg) for an adult of 50 years age is found directly from [23]. The tissue hydration rate α varies with TBW and mass density ρ for both the adult and child as:

$$\alpha = TBW\rho \tag{5}$$

The relative permittivity of a child's head as a function of child and adult biological tissue hydration rates is formulated as described in [24] and thus expressed as:

$$\varepsilon_{ch} = \varepsilon_{rw}^{\frac{\alpha_{ch}-\alpha_A}{1-\alpha_A}} \varepsilon_{rA}^{\frac{1-\alpha_{ch}}{1-\alpha_A}} \tag{6}$$

where α_{ch} and α_A are tissue hydration rates in children and adults, respectively. ε_{rw} is 74.3, the relative permittivity of water at 37°C, and ε_{rA} is the relative permittivity of tissues in the adult head, calculated using Eq. (2). The mass density does not change with age; the only parameters that change with age are tissue hydration rates and TBW. The following equations for intrinsic impedance and propagation constant of each layer are derived from dielectric characteristics of head layers.

$$\eta = 1 + j\sqrt{\frac{\pi f \mu}{\sigma}} \tag{7}$$

$$\gamma = \sqrt{j\omega\mu\left(\sigma + j\omega\varepsilon\right)} \tag{8}$$

where $\mu = \mu_0\mu_r$. The relative permeability of biological tissues is considered to be one, so $\mu_r = 1$. $\omega = 2\pi f$, $\varepsilon = \varepsilon_0\varepsilon_r$. μ is the permeability of a medium, and μ_0 is the permeability of free space.

For a four-layered adult or a child head model, taking a small region of the head and assuming it to be a laminated shield of three layers of skin-dry, bone-cortical, and brain gray matter, the shielding effectiveness of the head is formulated from transmission coefficient, reflection coefficients, and impedance at each layer using Transmission Line Method [25–27].

The transmission coefficient for power entering into brain white matter through the layers of skin, bone, and brain gray matter is expressed as:

$$p = \frac{16z_w\eta_s\eta_b\eta_g}{(z_w + \eta_s)(\eta_s + \eta_b)(\eta_b + \eta_g)(\eta_g + \eta_w)} \tag{9}$$

where z_w is the characteristic impedance of free space. η_s, η_b, η_g, and η_w are intrinsic impedances of skin, bone, gray matter, and white matter, respectively.

If the whole structure is assumed to be a transmission line, then the input impedances looking to the right of the bone and gray matter layers are expressed as:

$$z\left(l_1\right) = \eta_g\frac{\eta_w\ \cosh\left(\gamma_g l_3\right) + \eta_g\sinh\left(\gamma_g l_3\right)}{\eta_g\cosh\left(\gamma_g l_3\right) + \eta_w\sinh\left(\gamma_g l_3\right)} \tag{10}$$

$$z\left(l_2\right) = \eta_b\frac{\eta_g\ \cosh\left(\gamma_b l_2\right) + \eta_b\sinh\left(\gamma_b l_2\right)}{\eta_b\cosh\left(\gamma_b l_2\right) + \eta_g\sinh\left(\gamma_b l_2\right)} \tag{11}$$

where γ_b and γ_g are propagation constants of the wave in bone and gray matter, respectively, and l_2 and l_3 are the thicknesses of bone and gray matter.

The reflection coefficients of the electromagnetic wave at the interfaces of air-skin, skin-bone, and bone-gray matter are:

$$q_{as} = \frac{(\eta_s - z_w)\left[\eta_s - z\left(l_1\right)\right]}{(\eta_s + z_w)\left[\eta_s + z\left(l_1\right)\right]} \tag{12}$$

$$q_{sb} = \frac{(\eta_b - \eta_s)\left[\eta_b - z\left(l_2\right)\right]}{(\eta_b + \eta_s)\left[\eta_b + z\left(l_2\right)\right]} \tag{13}$$

$$q_{bg} = \frac{(\eta_g - \eta_b)(\eta_g - \eta_w)}{(\eta_g + \eta_b)(\eta_g + \eta_w)} \tag{14}$$

The total transmission coefficient of the radiated wave into human skin, bone, and gray matter for a four-layer adult or a child's head is expressed as:

$$T = p\left[\left(1 - q_{as}e^{-2\gamma_s l_1}\right)\left(1 - q_{sb}e^{-2\gamma_b l_2}\right)\left(1 - q_{bg}e^{-2\gamma_g l_3}\right)\right]^{-1}e^{(-\gamma_s l_1 - \gamma_b l_2 - \gamma_g l_3)} \tag{15}$$

Similar to the expressions in a four-layered model of the head, the expression for T can be extended to a seven-layer head model of an adult and a child as:

$$
\begin{aligned}
T = {} & p\left[\left(1 - q_{as}e^{-2\gamma_s l_1}\right)\left(1 - q_{sf}e^{-2\gamma_f l_2}\right)\left(1 - q_{fb}e^{-2\gamma_b l_3}\right)\right. \\
& \left.\left(1 - q_{bd}e^{-2\gamma_d l_4}\right)\left(1 - q_{dc}e^{-2\gamma_c l_5}\right)\left(1 - q_{cg}e^{-2\gamma_g l_6}\right)\right]^{-1} \\
& e^{\left(-\gamma_s l_1 - \gamma_f l_2 - \gamma_b l_3 - \gamma_d l_4 - \gamma_c l_5 - \gamma_g l_6\right)}
\end{aligned}
\tag{16}
$$

where p is the transmission coefficient for the power of wave entering into brain white matter through the layers of skin, fat, dura, CSF, bone, and brain gray matter. q_{sf}, q_{fb}, q_{bd}, q_{dc}, and q_{cg} are reflection coefficients of the wave at the interfaces of skin-fat, fat-bone, bone-dura, dura-CSF, CSF-gray matter, respectively. l_1, l_2, l_3, l_4, l_5, and l_6 are the thickness of skin, fat, bone, dura, CSF and gray matter, respectively. γ_s, γ_f, γ_d, and γ_c are propagation constants of skin, fat, dura and CSF layers in that order.

The shielding effectiveness in dB for a four-layered head model or a seven-layered head model for both adult and child heads can thus be formulated from the total transmission coefficient of the wave as:

$$
SE = -20\log_{10}|T| \tag{17}
$$

Case B: When the Shield is Considered: The second case considers an external shield when the mobile phone is in use. An external shield is positioned between the mobile phone and the skin of an adult's head, as in Fig. 4. The same shield can be positioned between a phone and child's head. The shield materials considered for analysis of transparent materials are:

- Single Shield of pure Silver (Ag) film.
- Single Shield of AgNW/PDDA composite film.
- Laminated Shield of AgNW/PDDA composite film with PEDOT:PSS polymer film coating.

The material characteristics are enumerated in detail in Table 1. In the DC conductivity of AgNW-PDDA from the table, l_1 and l_2 stand for thicknesses of AgNW layer and PDDA layer which are 100 nm and 2 nm, respectively. The DC conductivity of AgNW/PDDA composite film is obtained from the classical percolation theory [28]. The percolation threshold of a composite material in general can be calculated from

$$
\sigma_{dc} = \sigma_f\left(v_f - v_{fc}\right)^t \tag{18}
$$
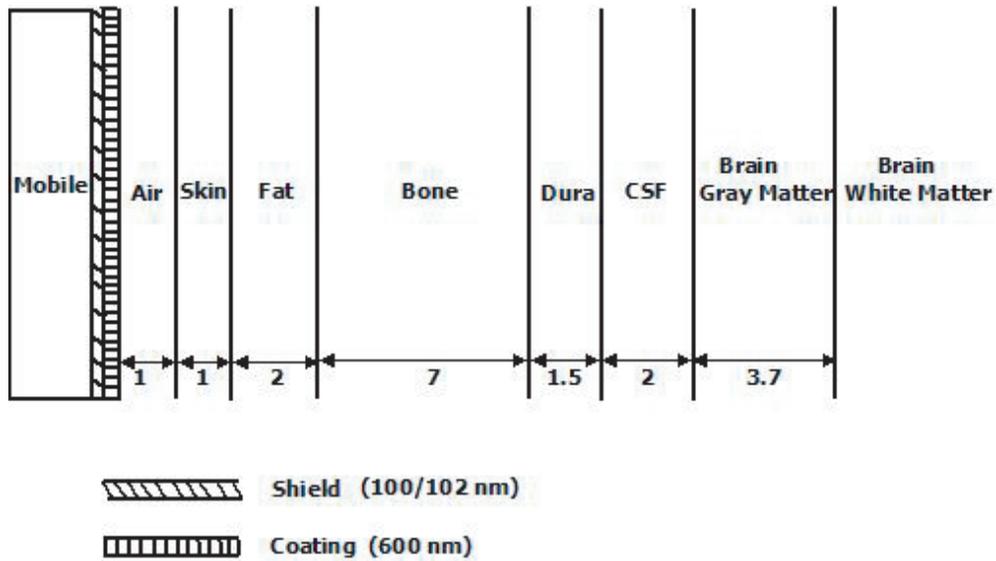
Figure 4. Positioning of shield along with coating for adult head model. Thickness of head tissues are in millimetres. Shield and coating thickness are in nanometres.

where σ_{dc} is the DC conductivity of the composite film, and σ_f and t are the electrical conductivity of filler and critical exponent, respectively. v_f is the volume fraction of filler, and v_{fc} is the percolation threshold needed to make an insulator behave as a conductor. The values of parameters for DC conductivity are incorporated from [29]. Using Eq. (18), the DC conductivity of AgNW/PDDA composite conductive film in Table 1 is obtained from parameters from [29] and the thickness of AgNW and PDDA layers considered. The DC conductivity and relative permittivity of pristine PEDOT:PSS films are referred from [30].

Table 1. Material characteristics of transparent thin films.

Material	Thickness (nm)	DC Conductivity (S/m)	Relative Permittivity
Ag film	100	6.3e7	1
AgNW-PDDA film	102	$3.34e - 5(l_1/l_2)$	1
PEDOT:PSS film	600	360000	5143

Using the dielectric properties of shield and from the theoretical analysis in the absence of a shield, the transmission coefficient of the radiated electromagnetic wave with Ag or AgNW/PDDA single shield, for a four-layer model, is given by:

$$T = p \left[\left(1 - q_{aSh}e^{-2\gamma_{sh}l_1}\right) \left(1 - q_{Sha}e^{-2\gamma_{fs}l_2}\right) \left(1 - q_{as}e^{-2\gamma_s l_3}\right) \left(1 - q_{sb}e^{-2\gamma_b l_4}\right) \right.$$
$$\left. \left(1 - q_{bg}e^{-2\gamma_g l_5}\right) \right]^{-1} e^{\left(-\gamma_{sh}l_1 - \gamma_{fs}l_2 - \gamma_s l_3 - \gamma_b l_4 - \gamma_g l_5\right)} \tag{19}$$

where q_{aSh} and q_{Sha} are reflection coefficients at air-shield and shield-air interfaces. Here, l_1, l_3, l_4, and l_5 are thicknesses of shield, skin, bone, and gray matter, respectively. l_3 is the gap distance of 1 mm between shield and skin layer of head. γ_{sh} and γ_{fs} are propagation constants of shield and free space in that order. The transmission coefficient of radiated EM wave with AgNW/PDDA/PEDOT:PSS laminated shield, for a four-layered head model, is:

$$T = p \left[\left(1 - q_{Sha}e^{-2\gamma_{Sh}l_1}\right) \left(1 - q_{Shc}e^{-2\gamma_{co}l_2}\right) \left(1 - q_{ca}e^{-2\gamma_{fs}l_3}\right) \right.$$
$$\left. \left(1 - q_{as}e^{-2\gamma_s l_4}\right) \left(1 - q_{sb}e^{-2\gamma_b l_5}\right) \left(1 - q_{bg}e^{-2\gamma_g l_6}\right) \right]^{-1}$$
$$e^{\left(-\gamma_{sh}l_1 - \gamma_{co}l_2 - \gamma_{fs}l_3 - \gamma_s l_4 - \gamma_b l_5 - \gamma_g l_6\right)} \tag{20}$$

where q_{Shc} and q_{ca} are reflection coefficients at shield-coating and coating-air interfaces. Here, l_1 and l_2 are the thicknesses of the shield and coating, respectively. l_3 is the gap distance of 1 mm between shield and skin. γ_{sh} and γ_{co} are propagation constants of shield and coating. Similar to the four-layer model with a shield positioned between the head and the mobile phone, the equations for T are formulated for a seven-layer adult or a child's head. Thus, the shielding effectiveness of a four or a seven-layered head with shield placed is estimated from Equation (17).

2.2. Computation of SAR from the Shielding Effectiveness of the Human Head

Since the SAR absorbed by the human head depends on the frequency of the source, in the proposed work, the SAR is estimated at each of the mobile frequencies of 800 MHz, 1800 MHz, 2.5 GHz, 3.6 GHz, 4.5 GHz, 5 GHz, and 6 GHz. The shielding effectiveness in dB of any barrier is defined for the electric field as the equation [31]:

$$SE = 20\log_{10}\frac{E_i}{E_t} \tag{21}$$

E_i is the incident electric field strength, and E_t is the electric field strength after coming out from the shield. The power density generated by the mobile phone can be calculated by using:

$$W_{\max} = \frac{P_t G_t}{4\pi d^2} \tag{22}$$

where P_t is the radiated power by mobile antenna taken to be 125 mW [32]. Assuming an isotropic antenna, G_t is considered one, and d is the minimum separation distance of 1 mm between the mobile phone and the head. Power density is expressed in W/m^2.

The impedance of head tissues at the air and skin interface remains fixed as 377 ohms. From the maximum power density, the induced or incident electric field in V/m is calculated as:

$$E_i = \sqrt{2W_{\max}\eta} \qquad (23)$$

For each of the shielding effectiveness values of the adult and child heads obtained above, the transmitted electric-field (E_t) is assessed for both without shield and with Ag film, AgNW/PDDA single shields, and AgNW/PDDA/PEDOT:PSS laminated shield using Eq. (21).

From the calculated E_t emerging out of the shield and entering the brain white matter tissue, the SAR (W/kg) absorbed by brain white matter in both the adult and child is computed with the formula:

$$SAR = \frac{\sigma E_t^2}{2\rho} \qquad (24)$$

σ is the conductivity of brain white matter, computed at different mobile frequencies, and ρ is the mass density of white matter, which is 1073 kg/m^3 [33].

3. RESULTS OF SIMULATION FOR SHIELDING EFFECTIVENESS OF HUMAN HEAD MODELS AND NUMERICAL COMPUTATION OF SAR

3.1. Shielding Effectiveness of Head Models without Shield

The shielding effectiveness for four and seven layers of both the adult and child's head models without the shield placed on the front side of the mobile phone is plotted against the frequency for the mobile frequency range 800 MHz to 6 GHz. The result is shown in Fig. 5.
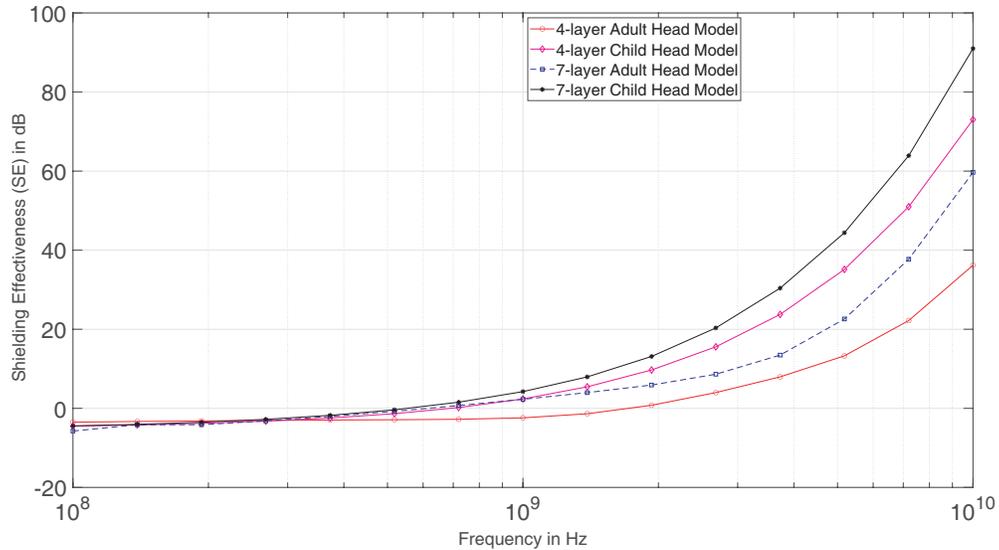
Figure 5. Simulation of shielding effectiveness for four and seven-layered adult and child head models without the shield.

The result obtained indicates that the shielding effectiveness for both four and seven-layer adult head models is less than for four and seven-layer child head models.

3.2. Shielding Effectiveness of Head Models with Shield

The shielding effectiveness for four and seven-layered head models of both adult and child with pure silver (Ag) transparent film as shield is plotted against the mobile frequencies. The shield thickness
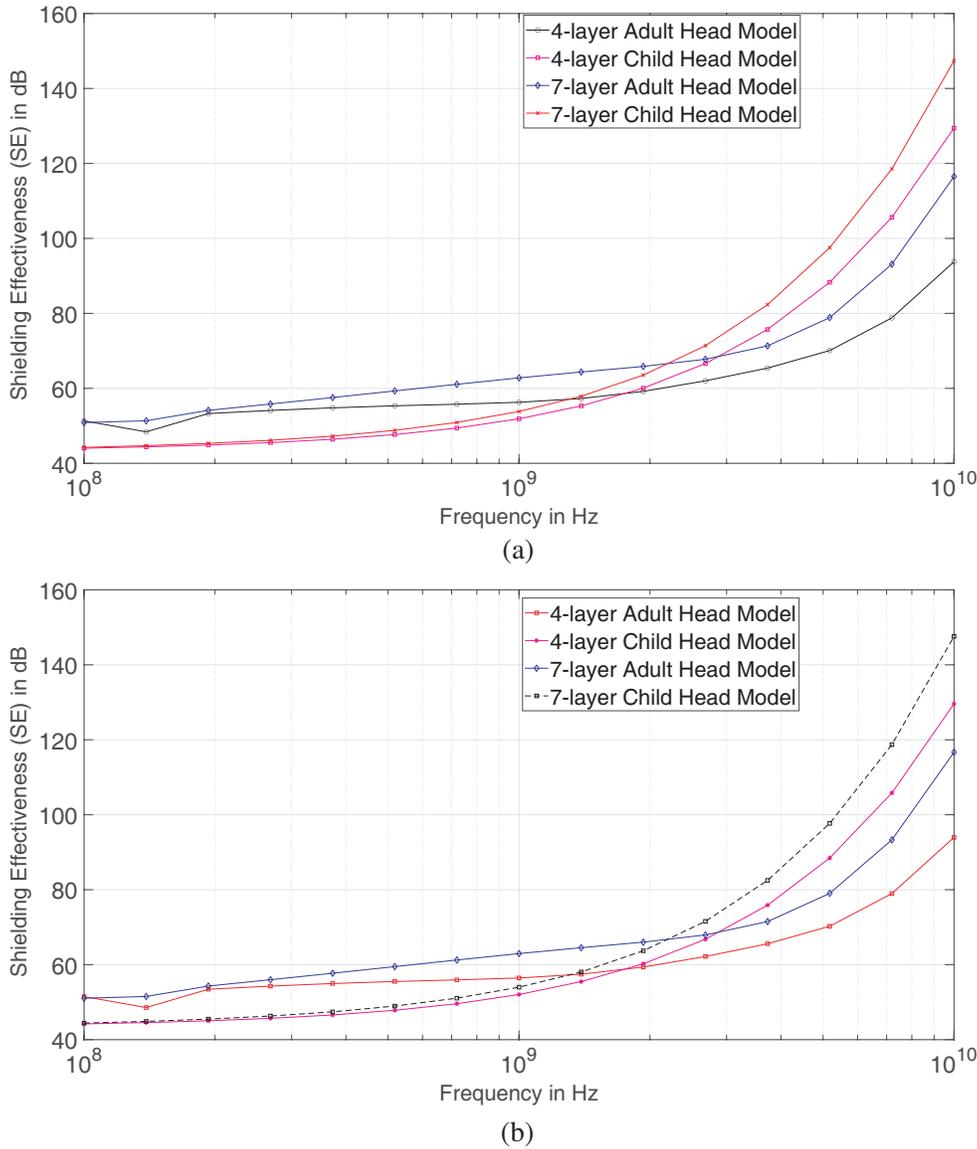
Figure 6. Simulations of shielding effectiveness for adult and child head models with four and seven layers using single shields of (a) Ag-film and (b) AgNW/PDDA film.

is considered as low as 100 nm. The graph against frequency for shielding effectiveness of all the four head models using Silver Nanowire-PDDA polymer transparent conducting composite film of thickness 102 nm is plotted. The thickness of PDDA layer is 2 nm. The results for both are shown in Figs. 6(a) and 6(b). The AgNW/PDDA single shield with PEDOT:PSS polymer as coating on top forms the laminated shield for AgNW/PDDA/PEDOT:PSS film. The thickness of the coating a material is considered to be 600 nm. The shielding effectiveness plot for the laminated shield using AgNW/PDDA and PEDOT:PSS coating material is simulated in Fig. 7. From the plots, it is observed that the seven-layered child head model achieves the highest shielding effectiveness with all the three transparent shields, and the shielding effectiveness being the lowest for the four-layered adult model.

3.3. Computation of SAR Absorbed by the Head Using Shielding Effectiveness

The SAR absorbed by the white matter tissue is theoretically attained from the difference in shielding effectiveness of the head without shield and with shield considered. SAR in W/kg is obtained using
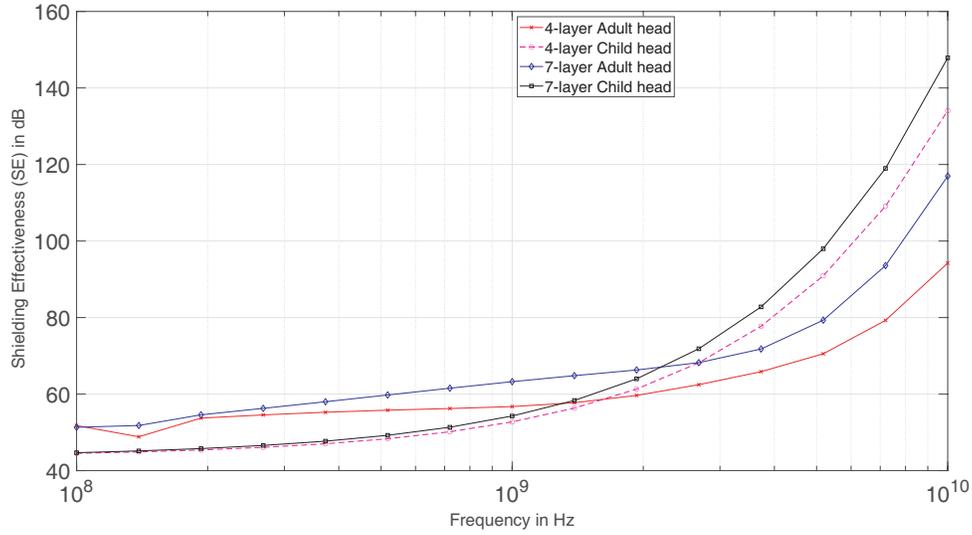
Figure 7. Simulation of shielding effectiveness for four and seven-layered adult and child head models with AgNW/PDDA/PEDOT:PSS laminated shield.

Table 2. SAR absorbed by brain white matter tissue in adult four-layered head model.

Frequency (GHz)	SAR absorbed by head without shield (W/kg)	SAR absorbed by head using Transparent shields (W/kg)		
		Ag-film	AgNW/ PDDA film	AgNW/PDDA/ PEDOT:PSS film
0.8	3644.43	0.005	0.0048	0.0045
1.8	3039.92	0.0043	0.0041	0.0039
2.5	2802.57	0.0052	0.0050	0.0047
3.6	1164.07	0.0020	0.00198	0.0018
4.5	734.71	0.0014	0.00138	0.00129
5.0	551.64	0.0011	0.00109	0.00101
6.0	276.57	0.0006	0.00058	0.00054

Table 3. SAR absorbed by brain white matter tissue in child four-layered head model.

Frequency (GHz)	SAR absorbed by head without shield (W/kg)	SAR absorbed by head using Transparent shields (W/kg)		
		Ag-film	AgNW/ PDDA film	AgNW/PDDA/ PEDOT:PSS film
0.8	9253.80	0.1089	0.104	0.09
1.8	3400.93	0.0321	0.0309	0.0243
2.5	1341.69	0.0109	0.0105	0.0077
3.6	265.64	0.00173	0.00166	0.0011
4.5	65.26	0.00036	0.00034	0.00021
5.0	29.32	0.000146	0.00014	0.000081
6.0	5.76	0.000024	0.000023	0.000012

the E_t values from Section 2.2. The SARs absorbed by the brain white matter tissue at various mobile frequencies for adult and child four-layered head models are represented in Table 2 and Table 3. Furthermore, the powers absorbed by the white matter tissue for adult and child head models consisting of seven layers are tabulated in Table 4 and Table 5, respectively.

The results clearly show that the specific absorption rate from the mobile phone is reduced considerably using Ag film, AgNW/PDDA, and AgNW/PDDA/PEDOT:PSS transparent films as shield between head and the mobile phone. The shielding effectiveness demonstrated by AgNW/PDDA/PEDOT:PSS laminated shield is the maximum among shields, and thus using this shield, the reduction of SAR absorbed by the adult or child head model is the maximum. A seven-layered adult or a child head model absorbs less radiation than a four-layered adult or a child head. At initial frequencies, the child model may have absorbed more SAR than the adult model, for both four and seven head layers as in literature. However, as the frequency is raised further till 6 GHz is reached, the SAR absorption declines to a lower extent. Comparatively, among all the head models from the results displayed, a seven layered child head model absorbs the least amount of radiation.

Table 4. SAR absorbed by brain white matter tissue in adult seven-layered head model.

Frequency (GHz)	SAR absorbed by head without shield (W/kg)	SAR absorbed by head using Transparent shields (W/kg)		
		Ag-film	AgNW/ PDDA film	AgNW/PDDA/ PEDOT:PSS film
0.8	1484.67	0.00134	0.00128	0.00120
1.8	913.82	0.00089	0.00086	0.00080
2.5	951.82	0.00110	0.00123	0.00116
3.6	344.33	0.00054	0.00052	0.00049
4.5	137.44	0.00028	0.00026	0.00025
5.0	73.39	0.000167	0.000160	0.000149
6.0	17.73	0.000047	0.000046	0.000043

Table 5. SAR absorbed by brain white matter tissue in child seven-layered head model.

Frequency (GHz)	SAR absorbed by head without shield (W/kg)	SAR absorbed by head using Transparent shields (W/kg)		
		Ag-film	AgNW/ PDDA film	AgNW/PDDA/ PEDOT:PSS film
0.8	6551.191	0.075	0.071	0.067
1.8	1627.79	0.0152	0.0146	0.0136
2.5	481.56	0.0039	0.0037	0.0035
3.6	60.575	0.00039	0.00038	0.00036
4.5	10.25	0.000056	0.000054	0.00005
5.0	3.74	0.0000189	0.0000181	0.000017
6.0	0.48	0.000002	0.0000019	0.0000018

4. CONCLUSION

The mathematical analysis of shielding effectiveness incorporating various transparent thin films as shields for head models of two different age groups is implemented in this research. The plane wave shielding effectiveness of single shields using flexible and transparent materials of pristine Ag film and AgNW with PDDA is presented here. The plane wave shielding effectiveness of laminated shield using transparent conductive composite film of AgNW with PDDA layer and PEDOT:PSS polymer as the coating layer is also presented. The coating layers of PDDA and PEDOT:PSS films not only prevent silver from oxidation but also are cost-effective. The SAR absorbed by the human head due to mobile phone exposure is numerically estimated both in the absence and presence of these transparent shields at various mobile frequencies. The SAR is computed from the shielding effectiveness of three shields obtained through theoretical analysis of Transmission Line Method. Theoretically, AgNW/PDDA/PEDOT:PSS laminated shield exhibited the highest shielding effectiveness of 100 dB for the child seven-layered head model. Among four-layered head prototypes, at 6 GHz, positioning AgNW/PDDA/PEDOT:PSS laminated shield between adult head and mobile phone reduced the SAR to 0.00054 W/kg from 276.57 W/kg when no shield was used. On the other hand, a child head model of four tissue layers at 6 GHz absorbed a minimal value of SAR 0.000012 W/kg incorporating the same shield in comparison with child head with no shield of 5.76 W/kg SAR. Among seven-layered head models, at a peak frequency of 6 GHz, placing the laminated shield made of Ag Nanowire/PDDA and PEDOT:PSS material reduced the SAR to 0.000043 W/kg from 17.73 W/kg with no shield in between mobile phone and the user's head. On the contrary, at 6 GHz mobile frequency, the child seven-layered head model absorbed a least radiation of 0.0000018 W/kg in the presence of the same laminated shield. Therefore, a seven layered child head with the Ag Nanowire/PDDA and PEDOT:PSS laminated transparent shield placed between the mobile smartphone and the head absorbs the least amount of RF radiation power level. All the RF radiation exposure levels obtained with the transparent conducting films from the results of the mathematical evaluation of SAR demonstrate that they comply with the FCC standardized SAR limit accepted worldwide. Hence, these results serve a good purpose for the betterment of present society, especially for children, where the alarming risks associated with the RF exposure of mobile smartphones are increasingly high with the utilization of these devices.

REFERENCES

1. Lak, A. and H. Oraizi, "Evaluation of SAR distribution in six-layer human head model," *International Journal of Antennas and Propagation*, Vol. 2013, 2013.

2. https://www.fcc.gov/general/specific-absorption-rate-sar-cellular-telephones.

3. He, L. and S. C. Tjong, "Nanostructured transparent conductive films: Fabrication, characterization and applications," *Materials Science and Engineering: R: Reports*, Vol. 109, 1–101, 2016.

4. Yang, Y., S. Chen, W. Li, P. Li, J. Ma, B. Li, X. Zhao, Z. Zhu, H. Chang, L. Xiao, H. Xu, and Y. Liu, "Reduced graphene oxide conformally wrapped silver nanowire networks for flexible transparent heating and electromagnetic interference shielding," *Acs Nano*, Vol. 14, No. 7, 8754–8765, 2020.

5. Wan, Y. J., X. Y. Wang, X. M. Lis, S. Y. Liao, Z. Q. Lin, Y. G. Hu, T. Zhao, X. L. Zeng, C. H. Li, S. H. Yu, P. L. Zhu, R. Sun, and C. P. Wong, "Ultrathin densified carbon nanotube film with "metal-like" conductivity, superior mechanical strength, and ultrahigh electromagnetic interference shielding effectiveness," *ACS Nano*, Vol. 14, No. 10, 14134–14145, 2020.

6. Chen, Y., L. Pang, Y. Li, H. Luo, G. Duan, C. Mei, W. Xu, W. Zhou, K. Liu, and S. Jiang, "Ultra-thin and highly flexible cellulose nanofiber/silver nanowire conductive paper for effective electromagnetic interference shielding," *Composites Part A: Applied Science and Manufacturing*, Vol. 135, 105960, 2020.

7. Alibakhshikenari, M., et al., "A comprehensive survey of "metamaterial transmission-line based antennas: Design, challenges, and applications," *IEEE Access*, Vol. 8, 144778–144808, 2020.

8. Alibakhshikenari, M., B. S. Virdee, and E. Limiti, "Compact single-layer traveling-wave antenna designusing metamaterial transmission lines," *Radio Science*, Vol. 52, No. 12, 1510–1521, 2017.

9. Alibakhshikenari, M., B. S. Virdee, A. Ali, and E. Limiti, "Extended aperture miniature antenna based on CRLH metamaterials for wireless communication systems operating over UHF to C-band," *Radio Science*, Vol. 53, No. 2, 154–165, 2018.

10. Alibakhshi-Kenari, M., et al., "A new miniature ultra wide band planar microstrip antenna based on the metamaterial transmission line," *2012 IEEE Asia-Pacific Conference on Applied Electromagnetics (APACE)*, 293–297, 2012.

11. Ojaroudi, P., et al., "Mobile-phone antenna array with diamond-ring slot elements for 5G massive MIMO systems," *Electronics*, Vol. 8, No. 5, 521, 2019.

12. Tamim, A. M., M. R. I. Faruque, M. U. Khandaker, M. T. Islam, and D. A. Bradley, "Electromagnetic radiation reduction using novel metamaterial for cellular applications," *Radiation Physics and Chemistry*, Vol. 178, 108976, 2021.

13. Belrhiti, L., F. Riouch, A. Tribak, J. Terhzaz, and A. M. Sanchez, "Investigation of dosimetry in four human head models for planar monopole antenna with a coupling feed for LTE/WWAN/WLAN internal mobile phone," *Journal of Microwaves, Optoelectronics and Electromagnetic Applications*, Vol. 16, 494–513, 2017.

14. Hout, S. and J. Y. Chung, "Design and characterization of a miniaturized implantable antenna in a seven-layer brain phantom," *IEEE Access*, Vol. 7, 162062–162069, 2019.

15. Drossos, A., V. Santomaa, and N. Kuster, "The dependence of electromagnetic energy absorption upon human head tissue composition in the frequency range of 300–3000 MHz," *IEEE Transactions on Microwave Theory and Techniques*, Vol. 48, No. 11, 1988–1995, 2000.

16. Rajagopal, B. and L. Rajasekaran, "SAR assessment on three layered spherical human head model irradiated by mobile phone antenna," *Human-centric Computing and Information Sciences*, Vol. 4, No. 1, 1–11, 2014.

17. Gabriel, S., R. W. Lau, and C. Gabriel, "The dielectric properties of biological tissues: III. Parametric models for the dielectric spectrum of tissues," *Physics in Medicine & Biology*, Vol. 41, No. 11, 2271, 1996.

18. http://niremf.ifac.cnr.it/docs/DIELECTRIC/AppendixC.html.

19. http://niremf.ifac.cnr.it/tissprop/htmlclie/htmlclie.php.

20. Ibrani, M., L. Ahma, and E. Hamiti, "The age-dependence of microwave dielectric parameters of biological tissues," *Microwave Materials Characterization*, Vol. 10, 51400, 2012.

21. Ibrani, M., L. Ahma, E. Hamiti, and J. Haxhibeqiri, "Derivation of electromagnetic properties of child biological tissues at radio frequencies," *Progress In Electromagnetics Research Letters*, Vol. 25, 87–100, 2011.

22. Fomon, S. J., F. Haschke, E. E. Ziegler, and S. E. Nelson, "Body composition of reference children from birth to age 10 years," *The American Journal of Clinical Nutrition*, Vol. 35, No. 5, 1169–1175, 1982.

23. Chumlea, W. C., S. S. Guo, C. M. Zeller, N. V. Reo, R. N. Baumgartner, P. J. Garry, J. Wang, R. N. Pierson, Jr., S. B. Heymsfield, and R. M. Siervogel, "Total body water reference values and prediction equations for adults," *Kidney International*, Vol. 59, No. 6, 2250–2258, 2001.

24. Wang, J., O. Fujiwara, and S. Watanabe, "Approximation of aging effect on dielectric tissue properties for SAR assessment of mobile telephones," *IEEE Transactions on Electromagnetic Compatibility*, Vol. 48, No. 2, 408–413, 2006.

25. Schulz, R. B., V. C. Plantz, and D. R. Brush, "Shielding theory and practice," *IEEE Transactions on Electromagnetic Compatibility*, Vol. 30, No. 30, 187–201, 1998.

26. Jayasree, P. V. Y., V. S. S. N. S. Baba, B. P. Rao, and P. Lakshman, "Analysis of shielding effectiveness of single, double and laminated shields for oblique incidence of EM waves," *Progress In Electromagnetics Research B*, Vol. 22, 187–202, 2010.

27. Dutta, P. K., P. V. Y. Jayasree, and V. S. S. N. S. Baba, "SAR reduction in the modelled human head for the mobile phone using different material shields," *Human-centric Computing and Information Sciences*, Vol. 6, No. 1, 1–22, 2016.

28. Ram, R., D. Khastgir, and M. Rahaman, "Electromagnetic interference shielding effectiveness and skin depth of poly (vinylidene fluoride)/particulate nano-carbon filler composites: Prediction of electrical conductivity and percolation threshold," *Polymer International*, Vol. 68, No. 6, 1194–1203, 2019.

29. Zhu, X., X. Juan, Q. Feng, Z. Yan, A. Guo, and C. Kan, "Highly efficient and stable transparent electromagnetic interference shielding films based on silver nanowires," *Nanoscale*, Vol. 12, No. 27, 14589–14597, 2020.

30. Wang, Y., C. Zhu, R. Pfattne, H. Yan, L. Jin, S. Chen, F. M. Lopez, F. Lissel, J. Liu, N. I. Rabiah, Z. Chen, J. W. Chung, C. Linder, M. F. Toney, B. Murmann, and Z. Bao, "A highly stretchable, transparent, and conductive polymer," *Science Advances*, Vol. 3, No. 3, e1602076, 2017.

31. Paul, C. R., *Introduction to Electromagnetic Compatibility*, John Wiley & Sons, New Jersey, 2006.

32. Rashid, T. B. and H. H. Song, "Analysis of biological effects of cell phone radiation on human body using specific absorption rate and thermoregulatory response," *Microwave and Optical Technology Letters*, Vol. 61, No. 6, 1482–1490, 2019.

33. Mohammed, B., K. Bialkowski, A. Abbosh, P. C. Mills, and A. P. Bradley, "Closed-form equation to estimate the dielectric properties of biological tissues as a function of age," *Bioelectromagnetics*, Vol. 38, No. 6, 474–481, 2017.